SAND2022-14285C

The Role of Stoichiometry in $Mn_{1-x}Zn_xFe_2O_4$ Ferrite Microwave Absorbers

Andrew S. Padgett, Sandia National Laboratories

Abstract:

As 5G technology moves higher into the microwave frequency regime the risk of coupling EM energy into susceptible electronic circuits grows [1]. Minimizing this interference is driving the need for compact, lightweight broadband absorbers to protect sensitive and high precision electronics. Manganese zinc ferrite ($Mn_{1-x}Zn_xFe_2O_4$) microparticles have previously been demonstrated to be magnetically lossy up to 10 GHz, the desired frequency regime, and have the potential to meet the energy density and attenuation performance needs [2]. However, optimizing the shielding effectiveness requires improved understanding of $Mn_{1-x}Zn_x$ stoichiometry and the dominant dielectric and magnetic absorption mechanisms for each stoichiometry [3]. This presentation discusses results, up to 10 GHz, from experimentally investigating the shielding effectiveness and TE011 loss attenuation of $Mn_{1-x}Zn_xFe_2O_4$ with a mean particle size of 30 microns, loaded to 50 volume percent in epoxy, and variation in x values from 0 to 1 in intervals of 0.1. Complex permeability and permittivity measurements were conducted to identify the peaks in the dielectric and magnetic loss tangents. An increase in absorption was observed in $Mn_{1-x}Zn_xFe_2O_4$ for x=0.4, 0.5, 0.6, and 0.7 compared with other stoichiometries at 2 and 5 GHz TE011 modes, and we discuss possible explanations based on resonance behavior in the loss tangents.

Experiment:

Mono-ferrite powders (i.e., $Mn_{1-x}Zn_xFe_2O_4$) powders obtained commercially from Trans-Tech, Inc. were used as filler in a flexible epoxy matrix and loaded to 50 volume percent to create the RF absorber materials for electrical and magnetic property testing. The flexible sheets were fabricated commercially by TPL, Inc. located in Albuquerque, NM and varied in thickness between 0.30 and 0.35 mm.

Loss attenuation was measured on TE_{011} modes at 1.111, 2.477, 5.157, and 10.011 GHz with four QWED split post dielectric resonators on Agilent Technologies PNA-L Network Analyzer N5235A 10MHz-50 GHz operating at 0 dBm with 1601 points in Log frequency. The loss attenuation is defined as the difference, in dB, between the peak power of the TE_{011} mode when the cavity is empty and when the sample is inserted. Differences in sample thickness are accounted for by reporting the results, in Figure 1, as loss attenuation per unit thickness (dB/mm).

Shielding effectiveness (SE) measurements were conducted using the same PNA-L Network Analyzer at 0 dBm with 1601 points with the Electro-Metrics Corporation EM-2108 SE measurements system. This is a coaxial type SE measurement where the reflection (R), transmission (T), and absorption (A) coefficients are defined in terms of the VNA s-parameters:

$$R = |s_{11}|^2$$
$$T = |s_{21}|^2$$
$$A = 1 - R - T = 1 - |s_{21}|^2 - |s_{11}|^2$$

Where A is determined by the fact that all power at a given frequency must be reflected, transmitted, or absorbed.

Complex permeability and permittivity were measured from 1-5 GHz with a GR900 coaxial type waveguide driven by a Keysight PNA Network Analyzer N5224A 10 MHz – 43.5 GHz. The s-parameters were converted to complex permittivity and permeability values with Keysight 85071E Materials Measurement Software. Measurements form 3-11 GHz were made with the Compass Technologies Group AMMP SP218 Spot Probe using 2-port Agilent Technologies PNA Network Analyzer N5224A 10 MHz-43.5 GHz.

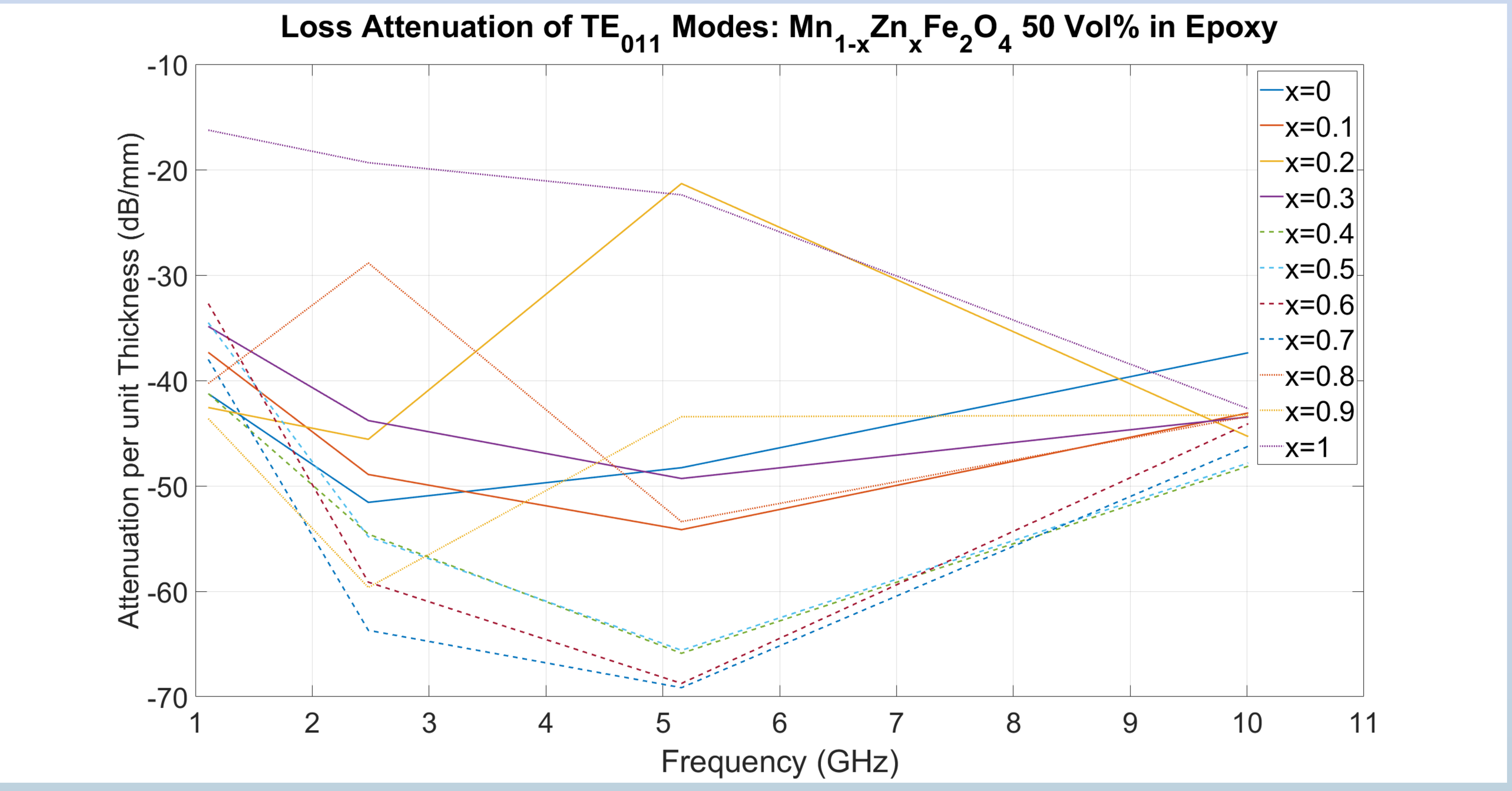

Figure 1. Loss attenuation of TE_{011} Modes between 1 and 10.1 GHz

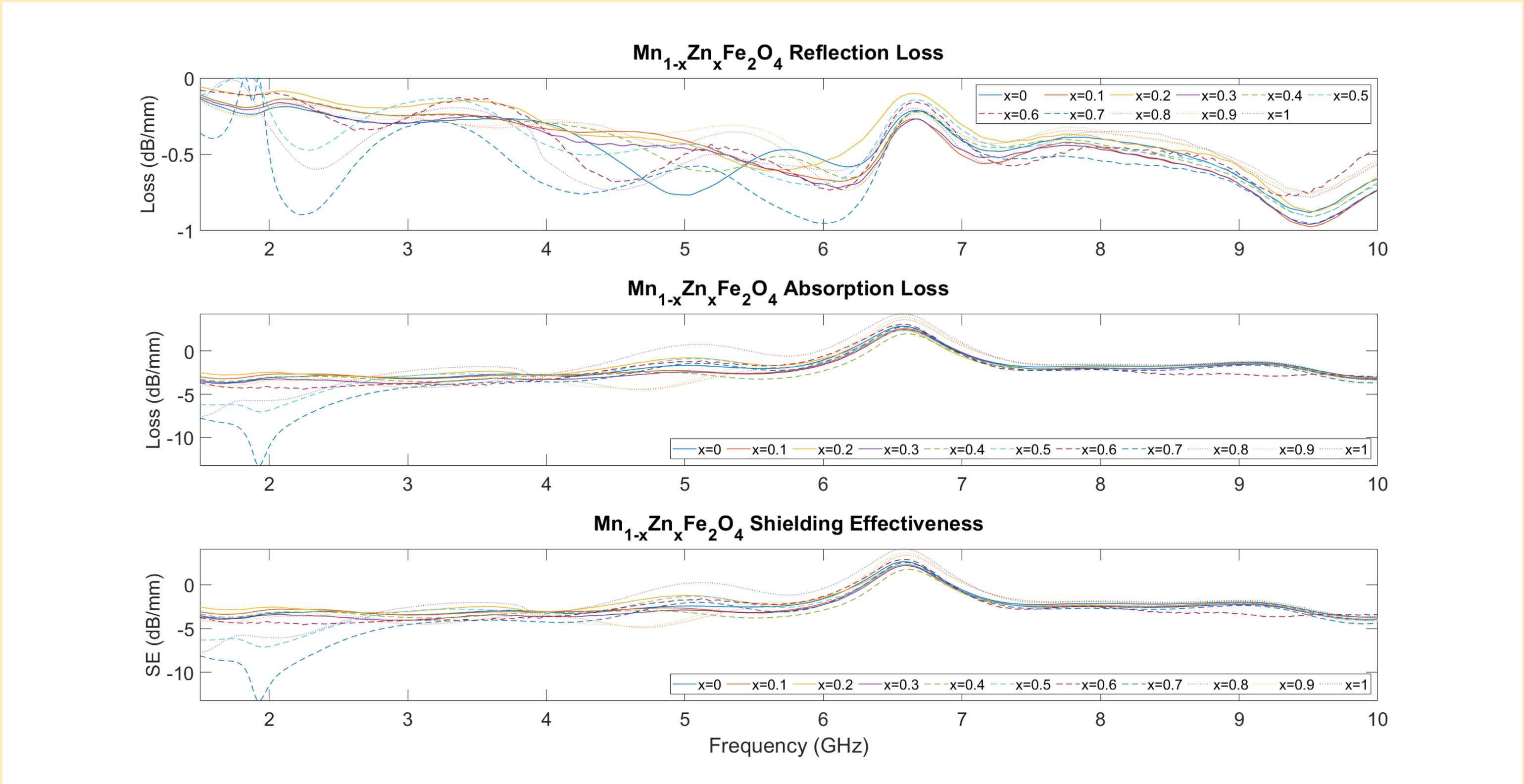

Figure 2. Reflection loss, absorption loss, and shielding effectiveness between 1.5 and 10 GHz

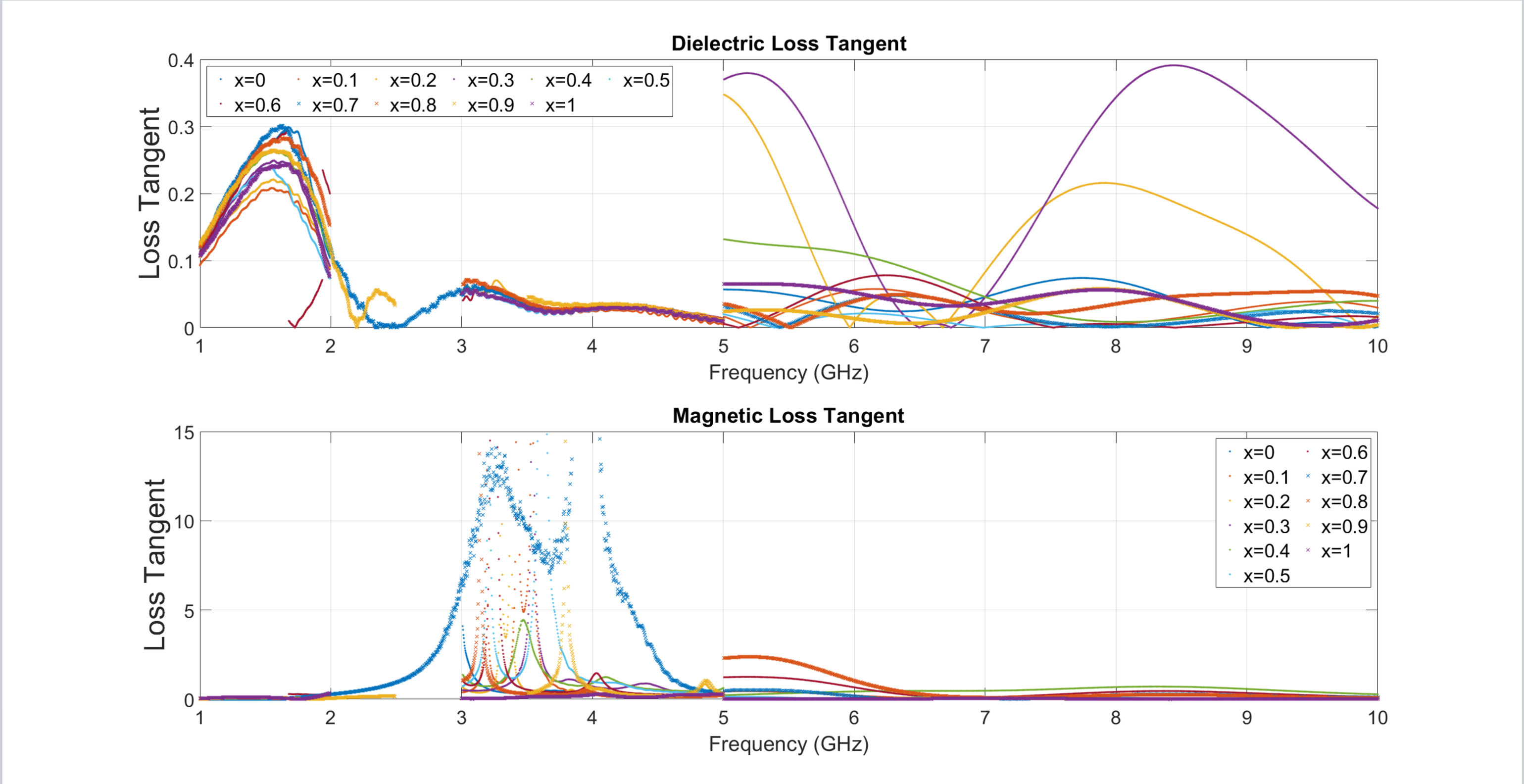

Figure 3. Dielectric and magnetic loss tangents between 1 and 10 GHz

Results:

The positive value for SE between 6 and 7 GHz in the bottom plot of Figure 2 is a consequence of the measurement method; two background measurements and one insertion loss measurement were required for each sample. The first background measurement, s_{11} and s_{21} with the empty EM-2108 connected, quantified scattering intrinsic to the EM-2108. Next, a washer and small disc of the material under test were placed over the outer and inner conductor of EM-2108 coaxial system to account for the impedance mismatch. Finally, a sample which filled both the dielectric air gap and the region of the inner and outer conductor was measured. Resonance behavior in the EM-2108 was accounted for in the background measurement, but new resonances were introduced with the sample measurement; consequently, the positive values of SE is a remnant of the measurement method and should be regarded as non-physical.

Permeability and permittivity measurements proved challenging for two reasons. The GR900 and spot probe yielded slightly different values at 5 GHz, where the data was united, leading to prominent discontinuities in the loss tangents. Additionally, the Nicholson-Ross-Weir method was used to convert the s-parameters to complex values, leading to divergences in the data where the sample thickness is an integer multiple of half wavelength inside the sample, which is dependent on the samples electrical length and therefore its complex permittivity [4]. Hence, ambiguous results, manifested as asymptotic discontinuities, appear if the approximate value of the complex permittivity in not known a priori. This manifested in the GR900 at about 3 GHz, where data has been subtracted in a 500 MHz band on either side of the discontinuity.

Discussion:

Manganese zinc ferrite (MZFO) has a spinel structure where Mn^{2+} or Zn^{2+} occupy either tetrahedral or octahedral sites within the lattice. Zn Ferrite is a normal, nonmagnetic spinel, where all Zn^{2+} cations occupy tetrahedral sites and all Fe^{3+} cations occupy octahedral sites; Mn ferrite is an inverse spinel, where all Mn^{2+} cations are located on octahedral sites [5]. As a consequence, $Mn_{1-x}Zn_xFe_2O_4$ transitions from an inverse spinel to normal spinel structure with increasing x, with mixed sates observed for intermediate stoichiometries [6]. The saturation magnetization of MZFO decreases linearly with increasing zinc content, but magnetic moment initially increases, reaching a maximum at x=0.4, before again beginning to decrease; MZFO transitions from ferromagnetic to paramagnetic for x≥0.6 at 300 K [7, 8]. The enhanced magnetic moment should translate to increased losses at ferromagnetic resonance near x=0.4, and we should see hysteresis losses disappear for x≥0.6. Paramagnetic materials do not form magnetic domains, so we should only see losses due to domain resonances in $Mn_{1-x}Zn_xFe_2O_4$ when x≤0.6. In sintered crystal ferrimagnetic samples, domain wall losses dominate in the kHz regime while ferromagnetic resonance (rotation) losses, indicates by a crossover between the real and imaginary components of the permeability, account for most energy dissipation in the MHz regime [9]. Our samples, however, are microparticle loaded polymers in which Snoek's limit is pushed to higher frequencies, such that we see magnetic relaxation losses well into the GHz regime [10].

In Figure 3, we observe magnetic loss tangents much greater than 1 between 2 and 5 GHz. The peaks for x=1, 0.9, and 0.7 strongly indicate ferromagnetic resonance behavior. Domain wall resonance occurs at lower frequencies than ferromagnetic resonance such that the lack of higher frequency peaks in the magnetic loss tangents eliminates them as the loss mechanism beyond 2 GHz. This would mean that our samples likely remain ferrimagnetic for x≥0.6, and there is no smooth transition from a normal to inverse spinel structure, with Mn and Zn cations partially occupying both octahedral and tetrahedral sites across the entire range of stoichiometries. This is unsurprising because the structure has been observed to strongly depends on the fabrication temperature [6]. In Figure 2, we see enhanced absorption for x=0.7 and 0.5 near 2 GHz which is likely due to magnetic, rather than dielectric, relaxations, as all samples, excluding x=0 and 0.2, show similar behavior (Figure 3, top) in their dielectric loss tangents in this frequency regime. Further, the large attenuation of the TE_{011} modes at 2.477 and 5.157 GHz (Figure 1) correspond to the large loss tangents exhibited by the x=0.4, 0.5, 0.6 and 0.7 stoichiometries near those frequencies. Notably, the x=0.7 stoichiometry shows the largest attenuation of the TE_{011} modes at 2.477 and 5.157 concomitant with exhibiting the largest and broades magnetic loss tangents in that frequency regime.

The dielectric properties of MZFO composites have been well characterized in the microwave regime [2] and its frequency dependent behavior is well understood [11]. By maintain a fixed volume fraction (50 vol%) we can observe, in Figure 3, the frequency dependence and bandwidth of the dielectric loss as a function of stoichiometry. The large bandwidth of the loss peaks, specifically for the cases x=0.2 and 0.3, is consistent with previous results [2] and consistent with expectation given that Mn is the main contributor to dielectric loss [11]. What is of much greater interest is the appearance of multiple dielectric loss peaks between 1 and 10 GHz for a single stoichiometry. This could be a consequence of uncertainties in the measurements introduced by the Nicholson-Ross Weir method used to extract the permeability and permittivity values, indication of structural variation for a given stoichiometry, or multiple loss mechanisms dominating in non-overlapping regimes. Unfortunately, the first case is the most likely. The significant discrepancies between the loss tangent values at 5 GHz, where the data from the two systems was united, indicates considerable uncertainty for one of the two measurements systems. Given the lack of increase in absorption in either the split post dielectric resonators or the EM-2108, Figure 1 and Figure 2, respectively, at the dielectric loss peaks measured by the spot probe, we believe the GR900 data to be more reliable.

Conclusion:

Our results indicate that 30 μm MZFO is a moderate to good magnetic absorber load material for hybrid microwave absorbers up to at least 5 GHz, with the x=0.5 and 0.7 stoichiometries providing the best performance with regard to absorption around 2 GHz and magnetic loss up to 5 GHz. Further, our results suggest that MZFO powder retains ferrimagnetic properties for all stoichiometries. This will be confirmed by performing vibrating sample magnetometry (VSM) measurements on all samples to look for hysteresis behavior. VSM will also provide magnetic saturation values for each stoichiometry indicating the maximum field intensities for which they will remain useful absorbers. Finally, we plan to investigate the role of MZFO particle size and load volume fraction on Snoek's limit and microwave shielding.

References:

[1] R. Dosoudil, M. Ušáková, J. Franek, J. Sláma, and V. Olah, "RF electromagnetic wave absorbing properties of ferrite polymer composite materials," *Journal of Magnetism and Magnetic Materials*, vol. 304, Issue 2, pp. e755-e757, 2006.

[2] D.Y. Kim, Y.C. Chung, T.W. Kang, and H.C. Kim, "Dependence of Microwave Absorbing Property on Ferrite Volume Fraction in MnZn Ferrite-Rubber Composites," *IEEE Transactions on Magnetics*, vol. 32, No. 2, 1996.

[3] N.N. Jiang, Y. Yang, Y.X. Zhang, J.P. Zhou, P. Liu, and C.Y. Deng, "Influence of zinc concentration on structure, complex permittivity and permeability of Ni–Zn ferrites at high frequency," *Journal of Magnetism and Magnetic Materials*, vol. 401, pp. 370-377, 2016.

[4] S. Arslanagić, T.V. Hansen, N.A. Mortensen, A.H. Gregersen, O. Sigmund, R.W. Ziolkowski, and O. Breinbjerg, "A Review of the Scattering-Parameter Extraction Method with Clarification of Ambiguity Issues in Relation to Metamaterial Homogenization," *IEEE Antenna and Propagation Magazine*, vol. 55, No. 2, 2013.

[5] A. Fairweather, F.F. Roberts, and A.J.E. Welch, "Ferrites," *Reports on Progress in physics*, vol. 15, No. 1, 1952.

[6] S. Sakurai, S. Sasaki, M. Okube, H. Ohara, and T. Toyoda, "Cation distribution and valence state in Mn– Zn ferrite examined by synchrotron X-rays," *Physica B*, vol. 403, Issue 19-20, pp. 3589-3595, 2008.

[7] R. L. Dhiman, V. Singh, S.P. Taneja, and K. Chandra, "Structural Investigation of Manganese Zinc Ferrites," *AIP Conference Proceedings*, vol. 2093, Issue 1, 2019.

[8] L.L. Ding, L.C. Xue, Z.Z. Li, S.Q. Li, G.D. Tang, W.H. Qi, L.Q. Wu, and X.S. Ge, "Study of cation distributions in spinel ferrites MxMn1-xFe2O4 (M=Zn, Mg, Al)," *AIP Advances*, vol. 6, Issue 10, 2016.

[9] F. Fiorillo, C. Beatrice, O. Bottauscio, and A. Manzin, "Approach to magnetic losses and their frequency dependence in Mn–Zn ferrites," *Applied Physics Letters*, vol. 89, Issue 12, 2006.

[10] R. Dosoudil, M. Ušáková, J. Franek, J. Sláma, and A. Grusková, "Particle Size and Concentration Effect on Permeability and EM-Wave Absorption Properties of Hybrid Ferrite Polymer Composites," *IEEE Transactions on Magnetics*, vol. 46, No. 2, pp. 436-439, 2010.

[11] K. Iwauchi, "Dielectric Properties of Fine Particles of Fe3O4 and Some Ferrites," *Japanese Journal of Applied Physics*, vol. 10, No. 11, 1971.

Acknowledgements:

I would like to thank Logan Robinett for conducting the split post dielectric resonator measurements and assisting with the complex permittivity and permeability characterization. I would also like to than Raymond Martinez for his assistance with sample preparation, purchases, and testing.